

# Identification of superlattice structure $cI16$ in the P-VI phase of phosphorus at 340 GPa and room temperature via x-ray diffraction

Toshiyuki Sugimoto,<sup>1</sup> Yuichi Akahama,<sup>1,\*</sup> Hiroshi Fujihisa,<sup>2</sup> Yoshiki Ozawa,<sup>1</sup> Hiroshi Fukui,<sup>1</sup> Naohisa Hirao,<sup>3</sup> and Yasuo Ohishi<sup>3</sup>

<sup>1</sup>Graduate School of Material Science, University of Hyogo, 3-2-1 Kouto, Kamigohri, Hyogo, 678-1297 Japan

<sup>2</sup>National Institute of Advanced Industrial Science and Technology (AIST), AIST Tsukuba Central 5, 1-1-1 Higashi, Tsukuba, Ibaraki 305-8565, Japan

<sup>3</sup>Japan Synchrotron Radiation Research Institute (JASRI), 1-1-1 Kouto, Mikazuki, Sayo-gun, Hyogo 679-5198, Japan

(Received 21 April 2012; published 30 July 2012)

The structural phase transitions of phosphorus (P) were investigated at pressures up to 340 GPa by a synchrotron radiation x-ray powder diffraction technique at room temperature. The transition from the simple hexagonal P-V to the P-VI phases was confirmed at 262 GPa. The results of full-profile Rietveld refinements indicate that the structure of the P-VI phase is a  $2 \times 2 \times 2$  superlattice of the bcc structure [ $cI16$  (space group:  $I-43d$ )], which is isotypic to high-pressure phases of Li and Na. This phase was found to be stable up to 340 GPa. The results have demonstrated the extension of structure refinement to a complex high-pressure phase above 300 GPa by the x-ray diffraction method.

DOI: [10.1103/PhysRevB.86.024109](https://doi.org/10.1103/PhysRevB.86.024109)

PACS number(s): 61.50.Ks, 62.50.-p, 61.05.cp, 64.70.K-

## I. INTRODUCTION

Recently, the study of crystal phase stability in highly compressed solids has progressed owing to the extension of the accessible pressure range through advances in the high-pressure x-ray diffraction technique, which uses a diamond anvil cell (DAC) and a synchrotron radiation (SR) x-ray source. The development of first-principles calculation methods has also given a boost to the progress. Various structural phase transitions under high-pressure conditions have been revealed in low- $Z$  elements, H<sub>2</sub>,<sup>1</sup> Li,<sup>2,3</sup> Na,<sup>4,5</sup> Al,<sup>6</sup> P,<sup>7-9</sup> Ca,<sup>10,11</sup> Sc,<sup>12-14</sup> and Ti.<sup>15,16</sup>

For P, which is a group 15 element, a five-stage structural phase transition has been observed at pressures up to 280 GPa, and unique crystal structures have been found at the higher-pressure range.<sup>7-9</sup> Black P, which is the most stable modification with the orthorhombic  $A17$  structure ( $Cmca$ , P-I) under ambient conditions,<sup>17</sup> is known to transform into the simple cubic (SC) phase ( $Pm-3m$ , P-III) at 10 GPa via the rhombohedral  $A7$  phase ( $R-3m$ , P-II).<sup>18</sup> The SC phase undergoes a structural transition to the simple hexagonal (SH) phase ( $P6/mmm$ , P-V) at 132 GPa through an intermediate phase (IM) with an incommensurate modulation ( $Cmmm(00\gamma)s00$ , P-IV).<sup>7-9</sup> The SH phase further undergoes a structural phase transition to the P-VI phase at 262 GPa, which is presently the highest pressure observed for a structural transition in elemental solids. A close-packed bcc ( $Im-3m$ ) structure has been proposed as a strong candidate for the P-VI phase.<sup>8</sup> However, the x-ray diffraction profile at 280 GPa, which was the maximum pressure in previous experiments, indicated that a fairly large amount of the SH phase still coexisted with the P-VI phase, and the possibility of other complex structures such as a superlattice of the bcc structure could not be ruled out. Therefore, to confirm the proposed structure, it is essential to observe a high-quality pattern of the P-VI single phase.

The successive structural phase transitions have attracted much interest in the theoretical modeling of the phase stability of group 15 elements under extreme conditions.<sup>19-26</sup> Total

energy calculations based on first-principles methods for the phase transitions have been in accordance with the SC-SH-bcc structure sequence experimentally observed up to 280 GPa.<sup>20-23,25</sup> The structure of the IM phase (P-IV) has also attracted special interest with respect to the mechanism of the SC-SH transition.<sup>21,23-26</sup> First-principles calculations by the metadynamics simulation method first predicted the incommensurate modulated structure in the IM phase.<sup>24</sup> More recent first-principles calculations have further proposed that the bcc structure becomes unstable above 280 GPa and transforms to a hcp structure ( $P6_3/mmc$ ) via an IM with a complex superlattice structure.<sup>25</sup>

The aim of the present study is to test the theoretically proposed high-pressure phase transitions above 280 GPa, as well as to check the proposed close-packed bcc structure. Herein, we present the results of x-ray powder diffraction analysis of P at pressures up to 340 GPa and report the unexpected finding that the P-VI phase has a distorted  $2 \times 2 \times 2$  superlattice structure of the bcc structure.

## II. EXPERIMENTAL

A DAC with a double bevel anvil geometry was used to generate ultrahigh pressure. The anvils had a loading axis along the [001] crystal direction, and the diameter of the flat face of the diamond anvils was 25  $\mu\text{m}$ . The first and second bevel diameters and angles were 250  $\mu\text{m}$  and 8.0° and 450  $\mu\text{m}$  and 15°, respectively. A rhenium (Re) metal sheet gasket with a thickness of 250  $\mu\text{m}$  was preindented to 6  $\mu\text{m}$  and was holed to obtain a sample chamber of 12  $\mu\text{m}$  in diameter. The starting material, black P, was finely ground from a high-purity single crystal<sup>27</sup> and placed into the hole of the Re metal gasket without using a pressure medium. In the experiment, the pressure in the sample chamber was estimated from the pressure shift of the Raman band edge of the diamond anvils, which was calibrated using a Pt scale.<sup>28</sup> Pressure uncertainty was estimated to be within  $\pm 3\%$ . Raman spectra were obtained using a micro-optical spectroscopic system.<sup>29</sup>

The excitation source was a He-Ne laser of wavelength 632.8 nm.

X-ray diffraction experiments at high pressure were conducted at room temperature by an angle dispersive method using a monochromatic SR source ( $E = 30$  keV) on the BL10XU beamline at SPring-8. A compound refractive lens made from glassy carbon and SU-8 polymer was used to focus the x ray on the small sample in order to overcome the low scattering efficiency due to the relatively low- $Z$  element P. Details of the beamline and the x-ray focusing system have been described elsewhere.<sup>30</sup> The full width of half maximum of the x-ray beam was a  $5 \times 5 \mu\text{m}^2$ . The beam profile was shaped up using a Pt pinhole collimator of  $10 \mu\text{m}$  in diameter placed just before the DAC. The stress diamond emitted light when irradiated with the x rays. From microscopic observation, we could then see the position of the x-ray direct beam as a light spot on the culet. The x-ray luminescence from the culet of the stressed diamond thus enabled precise alignment of the x-ray beam on the sample. The mechanism of the luminescence is under investigation at present. Diffraction patterns were recorded on an image plate detector. The  $2\theta$ -intensity profiles were obtained via an integration of the recorded two-dimensional diffraction images.<sup>31</sup>

### III. RESULTS AND DISCUSSION

Powder x-ray diffraction profiles of P were collected at pressures up to 340 GPa. The structural transition from the P-V(SH) to P-VI phases was reproduced with the appearance of a new reflection around  $2\theta = 14^\circ$  in the profile at 262 GPa, whereas the transitions from the P-III(SC) to P-IV(orthorhombic) phases and further to the PV(SH) phase were observed over a lower-pressure range. The transition to the P-VI phase was quite sluggish, and the P-V phase coexisted with the P-VI phase over a wide pressure region between 262 and 322 GPa. The profile of the P-VI single phase was recorded above 328 GPa, and this phase was stable at least up to 340 GPa.

The diffraction profile of the P-VI phase at 340 GPa is shown in Fig. 1. The background Compton scattering from the diamond anvils was numerically subtracted. From the diffraction image shown in the inset, it was found that the Debye rings are smooth and homogeneous, despite the limited amount of the sample. In the profile, new weak diffraction peaks were observed, in addition to the diffraction peaks of the bcc structure, which correspond to the 110, 200, 211, and 220 reflections. It also includes extra diffraction peaks with a relatively weak intensity and a wide peak width from the Re gasket. The new weak peaks suggest that the P-VI phase has a superlattice of the bcc structure rather than the bcc structure.

All diffraction peaks, except for peaks from the Re gasket, were completely indexed by a cubic lattice. The lattice parameter was estimated as  $a = 4.778(2)$  Å. This value is twice that of the previously proposed bcc structure.<sup>8</sup> These indices showed systematic absences that are consistent with the space group  $I-43d$  under general conditions for the allowed reflections:  $h + k + l = 2n$  for  $(hkl)$ ,  $2h + l = 4n$ , and  $l = 2n$  for  $(hhl)$ , where  $h$ ,  $k$ , and  $l$  are Miller indices. Therefore, the cubic cell was considered to be a  $2 \times 2 \times 2$  superlattice of

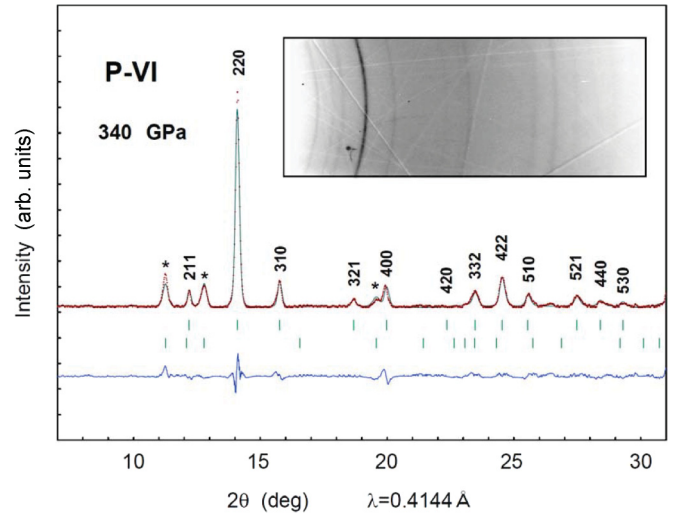


FIG. 1. (Color online) The observed diffraction profile of phosphorus phase VI at 340 GPa (dots) and the calculated profile (curve) after the Rietveld refinement. The profile was collected using an x-ray wavelength of 0.4144 Å. The asterisks represent peaks from the Re gasket. The up and down tick marks show the calculated peak positions for the  $I-43d$  structure ( $a = 4.778(2)$  Å) with 16 P atoms in the  $16c$  Wyckoff positions  $(x, x, x)$  and the hcp-Re, respectively. The differences between the observed and calculated profiles are shown below the tick marks. The obtained value of  $x$  was 0.0244(3) with a reliability factor of  $R_{wp} = 14.3\%$ . The Sasa-Uda preferred orientation function (Ref. 40) was used for fitting to the pattern of the Re gasket. The inset in the figure presents a part of the diffraction image.

the bcc structure containing 16 P atoms. The absence of a 420 peak satisfied the special condition of the  $16c$  Wyckoff positions  $(x, x, x)$ :  $h + k + l = 4n$  when  $h$  and  $k$  (and  $l$ ) =  $2n$ . The 420 peak is the only reflection in the observed range of data that is able to discriminate between the  $16c$  site and other sites. This site is also the only solution that provides a sensible density in the volume-pressure relationship (as will be seen in Fig. 3). In the initial analysis, the relative intensities were well explained as the  $I-43d$  structure with 16 P atoms in the  $16c$  Wyckoff positions  $(x, x, x)$ . Based on the Rietveld refinements of the profile using the computer program RIETAN,<sup>32</sup> the positional parameter  $x$  was estimated to be 0.0244(3) with a reliability factor of  $R_{wp} = 14.3\%$  for the full profile and  $R_I = 4.9\%$  for the integrated intensity of the P-VI phase. The simulated diffraction profile is shown by the solid line in Fig. 1. Refinement was performed in combination with the pattern of the Re gasket, which showed a strong preferred orientation.

The relatively large value of  $R_{wp}$  mainly results from the effect of uniaxial stress. Owing to this effect, the  $d$  spacings of the diffraction peaks for a cubic lattice often show a systematic deviation from that under hydrostatic conditions. In Fig. 2, the lattice constant  $a_{hkl}$  calculated from the main diffraction peaks at 340 GPa is plotted as a function of  $3(1 - 3 \sin^2 \theta) \Gamma(hkl)$ , where  $\Gamma(hkl) = (h^2 k^2 + k^2 l^2 + l^2 h^2) / (h^2 + k^2 + l^2)$ . The  $\Gamma$  plot indicates the above-mentioned effect, although it is difficult to estimate the uniaxial stress component.<sup>33</sup> The deviations are clear in Fig. 1, where it can be seen from the difference plot that the strong 220 is displaced to higher

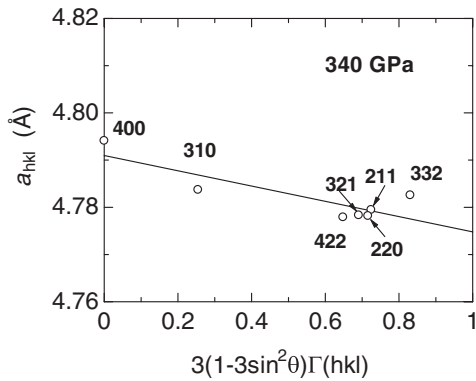


FIG. 2. The lattice constant calculated from the main reflection lines is plotted as a function of  $3(1 - 3 \sin^2 \theta) \Gamma(hkl)$ , where  $\Gamma(hkl) = (h^2 k^2 + k^2 l^2 + l^2 h^2) / (h^2 + k^2 + l^2)$ . The  $\Gamma$ -plot provides evidence for the uniaxial effect in the P-VI phase.

$2\theta$  and the 310 and 400 are displaced to lower  $2\theta$ . These displacements made the value of  $R_{wp}$  large. Therefore, in order to test the positional parameter  $x$  and its standard deviation obtained from the Rietveld refinements, the structure refinement using SHELXL97<sup>34</sup> was carried out on the basis of observed integrated intensities, taking into account the multiplicity of each reflection. The integrated intensities are listed in Table I. The estimated  $x$  and its standard deviation were 0.0244(7) with  $R = 5.9\%$  and showed in good agreement with the results of the Rietveld refinements.

Figure 3 shows the  $I-43d$  structure. The structure is a body-centered unit cell with 16 atoms (Pearson's notation  $cI16$ ). The  $cI16$  structure is a  $2 \times 2 \times 2$  superlattice of the bcc structure, which can be viewed as an arrangement of atomic chains running parallel to the four differently oriented body diagonals of a cubic lattice. The complex structure is derived by displacing the linear atomic chains with respect to each other along the  $\langle 111 \rangle$  directions, as shown in Fig. 3(b). In these chains, each P atom has two nearest-neighbor atoms at a distance of 2.068(1) Å at 340 GPa. Each P atom also has six second nearest-neighbor atoms with a distance of 2.094(1) Å,

TABLE I. The  $2\theta$ , relative integrated intensity  $I(\text{obs})$ , and multiplicity  $m$  of the observed diffraction peaks, and the calculated intensity  $I(\text{cal})$ .

| No. | $h$ | $k$ | $l$ | $2\theta$ | $I(\text{obs})$ | $I(\text{cal})$ | $m$ |
|-----|-----|-----|-----|-----------|-----------------|-----------------|-----|
| 1   | 2   | 1   | 1   | 12.198    | 8819            | 6558            | 24  |
| 2   | 2   | 2   | 0   | 14.093    | 100000          | 90200           | 12  |
| 3   | 3   | 1   | 0   | 15.767    | 14574           | 14330           | 24  |
| 4   | 3   | 2   | 1   | 18.680    | 3865            | 5029            | 48  |
| 5   | 4   | 0   | 0   | 19.982    | 12052           | 15064           | 6   |
| 6   | 4   | 2   | 0   | 22.369    | 0               | 0               | 24  |
| 7   | 3   | 3   | 2   | 23.476    | 6931            | 7954            | 24  |
| 8   | 4   | 2   | 2   | 24.536    | 21579           | 22209           | 24  |
| 9   | 5   | 1   | 0   | 25.555    | 2765            | 2722            | 24  |
| 10  | 4   | 3   | 1   | 25.555    | 5531            | 5540            | 48  |
| 11  | 5   | 2   | 1   | 27.486    | 7827            | 7174            | 48  |
| 12  | 4   | 4   | 0   | 28.406    | 4618            | 4051            | 12  |
| 13  | 5   | 3   | 0   | 29.299    | 3638            | 3472            | 24  |

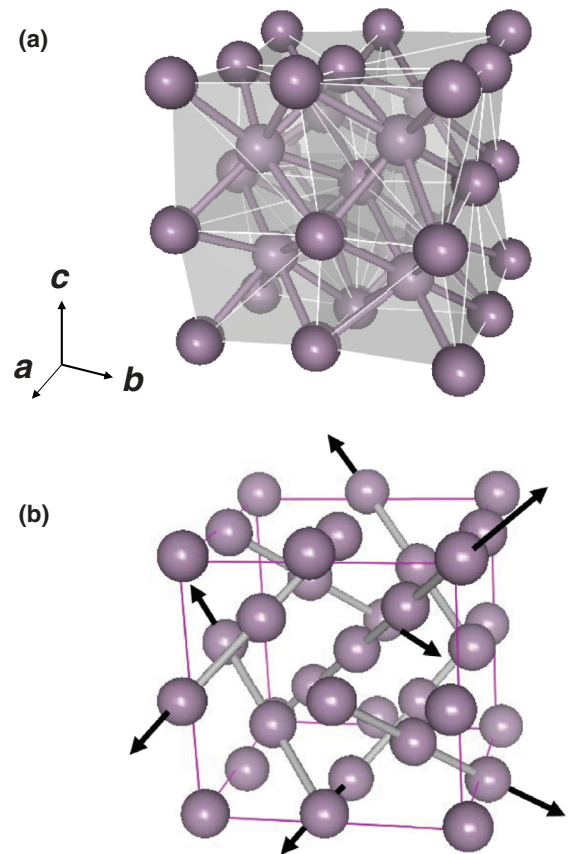


FIG. 3. (Color online) The structure model of the  $I-43d$  structure of the P-VI phase at 340 GPa. (a) The structure can be considered to be a  $2 \times 2 \times 2$  superlattice of the bcc structure with a small displacement of the position of the atoms along the space diagonal. Each P atom has a pseudocoordination number of 8; there are two nearest-neighbor atoms at a distance of 2.068(1) Å and six second nearest-neighbor atoms at a distance of 2.094(1) Å. (b) The different displacements of nearest-neighbor chains along the  $\langle 111 \rangle$  directions are illustrated.

which is 1.3% longer than the intrachain distance. Each atom has a pseudocoordination number of  $8 = 2 + 6$ . The  $x$  value did not show any detectable change with pressure in the region 328–340 GPa.

The relationship between pressure and atomic volume is illustrated in Fig. 4 along with our previous results.<sup>7-9</sup> Present results are in good agreement with the previous results. The P-V phase coexists with the P-VI phase over a wide pressure region. From the results, the volume reduction ( $-\Delta V$ ) at the transition pressure 262 GPa was estimated to be  $0.30 \text{ \AA}^3$ , which corresponds to 4.2% of the volume at the transition pressure. Although the SH phase has the same pseudocoordination number as the P-VI phase, i.e.,  $6 + 2$ , the ideal packing fraction of the atoms for the SH lattice is 0.605. The  $cI16$  structure is approximately the bcc structure with the packing fraction of 0.680. The large volume reduction rate of 4.2% would be due to an increase in the atomic packing fraction. The discontinuous volume change indicates that the transition is of the first order. The mechanism of the structural transition is not explained as a martensitic transformation by a lattice distortion with simple displacement of P atoms within a unit cell, such as is

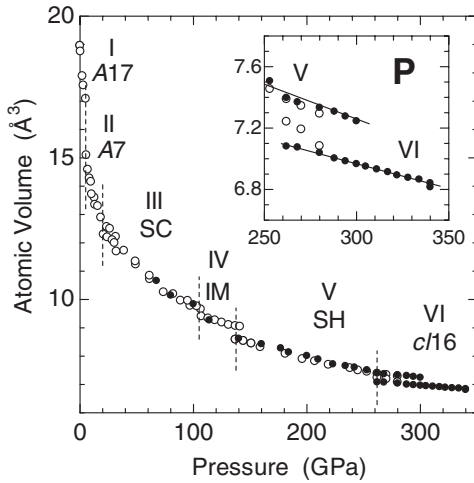


FIG. 4. The pressure dependence of the atomic volume of phosphorus. The solid and open circles correspond to the present results and our previous results (Refs. 7–9), respectively.

the case for other structural transitions of P<sup>7,35</sup> that occur in the lower-pressure range. Therefore, the transition should be accompanied by diffusion of the atoms. The observation that the transition to the P-VI phase was considerably sluggish compared with the other transitions of P, is likely due to the kinetics of the phase transition. With increasing pressure, the atomic volume decreases and at the highest pressure of 340 GPa the volume reaches  $6.8 \text{ \AA}^3$ , which corresponds to 36% of  $V_0$  ( $18.96 \text{ \AA}^3$ ) at ambient pressure.

The *cI16* structure was observed in the high-pressure phases of the elemental materials of alkali metals Li<sup>2</sup> and Na.<sup>4,5</sup> The values of the positional parameter  $x$  for Li and Na are 0.047–0.055 and 0.044, respectively, and are large compared with those of the P-VI phase. In the case of  $x > 0.0366$ , i.e.,  $(1 - 1/\sqrt{2})/8$ , each atom has three nearest-neighbor atoms and two second nearest-neighbor atoms. Thus, the coordination relationship of the atoms is different from that of the structure of the P-VI phase. Even so, it is interesting that the *cI16* structure appears in P, which atom has different electron configuration from alkali metal atoms.

In all previous total energy calculations for P phases, the bcc structure becomes energetically more stable than the SH structure in the higher-pressure range.<sup>20–23,25</sup> Because the *cI16* structure can be interpreted as a slightly distorted bcc structure, the theoretical results would be basically consistent with the present experimental results. The present results suggest that the total energy of the crystal decreases with the atomic displacement along the (111) directions. Indeed, recent theoretical calculations of the phonon dispersion relationship for the bcc structure have revealed that the transverse mode at the N point in the Brillouin zone softens with increasing pressure, and above 285 GPa, the frequency of the mode becomes imaginary.<sup>22,25</sup> In addition, they suggest that such dynamical instability of the bcc structure induces the phase transition to a bcc superlattice structure. However, the proposed structure is composed of a  $\sqrt{2} \times \sqrt{2} \times 1$  supercell of the bcc structure<sup>25</sup> and is different from the *cI16* structure. Nevertheless, the present experimental results support the

theoretical result that the bcc structure is unstable at ultrahigh pressures.

In this study, P showed the following structural sequence; A17(*Cmca*)-A7(*R-3m*)-SC(*Pm-3m*)-IM(*Cmmm(00\gamma)s00*)-SH(*P6/mmm*)-*cI16(I-43d)*. Other group 15 elements including As, Sb, and Bi are known to show a different common structural sequence of phase transitions under higher pressures: A7-(SC)-Ba-IV-type-bcc.<sup>36–39</sup> Namely, after passing through the SC structure, P and the other group 15 elements show a different structural sequence. This difference probably results from the fact that in the P atom, there are no *d* electrons in the core. In general, it is well known that the *s-d* transition plays a major role in structural phase transitions at higher pressures. That is, under highly compressed conditions, the higher-lying *d* bands hybridize with the *sp* bands, and *sp* electrons transfer partly to the *d* states. In fact, recent first-principles calculations have demonstrated an effectively higher *sp-d* hybridization with the states at and below the Fermi level in P, compared with the other group 15 elements. This is due to the absence of the *d* electrons in the core because the *3d* valence orbitals of P are not constrained by repulsive core orthogonality requirements.<sup>25</sup> Such highly hybridized *3d* bands probably play a role in the stability of unique and/or complex crystal structures.

In the case of P, the pressure-induced successive structural transitions are accompanied by an increase in the packing fraction of the atoms and/or the coordination number of the atoms.<sup>7,35</sup> Therefore, the transition to a structure with a higher packing fraction, such as the hcp and fcc structures would be expected at higher pressures. Indeed, recent first-principles calculations have predicted the phase transition to the hcp structure at 346 GPa.<sup>25</sup> For the experimental verification of this prediction, more accurate information about the transition pressure is indispensable and recalculations starting at the *cI16* structure are required.

#### IV. CONCLUSION

This study confirmed a previously proposed structural phase transition of P at 262 GPa. On the basis of the diffraction profile of the P-VI single phase, the structure of the highest-pressure phase of P was determined to be a body-centered unit cell with the 16 atoms (with the space group *I-43d* or in Pearson's notation, *cI16*), that is, a superlattice of the simple bcc structure. The result of the present experiment demonstrated that for low-*Z* elemental materials, it is possible to determine a complex structure even at ultrahigh pressures beyond 300 GPa. Although the structural stability of P at ultrahigh pressures has been theoretically investigated, a total energy calculation for the *cI16* structure has not been performed yet. Thus, the phase transition to the P-VI phase would be a good target for state-of-the-art first-principles calculation methods.

#### ACKNOWLEDGMENTS

The SR experiments were performed at SPring-8 with the approval of the Japan Synchrotron Radiation Research Institute (JASRI; Proposals No. 2011A1153 and No. 2011B1104).

- \*Corresponding author: akahama@sci.u-hyogo.ac.jp
- <sup>1</sup>Y. Akahama, M. Nishimura, H. Kawamura, N. Hirao, Y. Ohishi, and K. Takemura, *Phys. Rev. B* **82**, 060101(R) (2010).
- <sup>2</sup>M. Hanfland, K. Syassen, N. E. Christensen, and D. L. Novikov, *Nature (London)* **408**, 174 (2000).
- <sup>3</sup>C. L. Guillaume, E. Gregoryanz, O. Degtyareva, M. I. McMahon, M. Hanfland, S. Evans, M. Guthrie, S. V. Sinogeikin, and H.-K. Mao, *Nat. Phys.* **7**, 211 (2011).
- <sup>4</sup>K. Syassen, in *High Pressure Phenomena, Proceedings of the International School of Physics*, edited by R. J. Hemley, G. L. Chiarotti, M. Bernasconi, and L. Ulivi (IOS Press, Amsterdam, 2002), pp. 266–268.
- <sup>5</sup>M. I. McMahon, E. Gregoryanz, L. F. Lundegaard, I. Loa, C. Guillaume, R. J. Nelmes, A. K. Kleppe, M. Amboage, H. Wilhelm, and A. P. Jephcoat, *Proc. Natl. Acad. Sci., USA* **104**, 17297 (2007).
- <sup>6</sup>Y. Akahama, M. Nishimura, K. Kinoshita, H. Kawamura, and Y. Ohishi, *Phys. Rev. Lett.* **96**, 045505 (2006).
- <sup>7</sup>Y. Akahama, M. Kobayashi, and H. Kawamura, *Phys. Rev. B* **59**, 8520 (1999).
- <sup>8</sup>Y. Akahama, H. Kawamura, S. Carlson, T. Le Bihan, and D. Häussermann, *Phys. Rev. B* **61**, 3139 (2000).
- <sup>9</sup>H. Fujihisa, Y. Akahama, H. Kawamura, Y. Ohishi, Y. Gotoh, H. Yamawaki, M. Sakashita, S. Takeya, and K. Honda, *Phys. Rev. Lett.* **98**, 175501 (2007).
- <sup>10</sup>H. Fujihisa, Y. Nakamoto, K. Shimizu, T. Yabuuchi, and Y. Gotoh, *Phys. Rev. Lett.* **101**, 095503 (2008).
- <sup>11</sup>W. L. Mao, L. Wang, Y. Ding, W. Yang, W. Liu, D. Y. Kim, W. Luo, R. Ahuja, Y. Meng, S. Sinogeikin, J. Shu, and H. K. Mao, *Proc. Natl. Acad. Sci. USA* **107**, 9965 (2010).
- <sup>12</sup>Y. Akahama, H. Fujihisa, and H. Kawamura, *Phys. Rev. Lett.* **94**, 195503 (2005).
- <sup>13</sup>H. Fujihisa, Y. Akahama, H. Kawamura, Y. Gotoh, H. Yamawaki, M. Sakashita, S. Takeya, and K. Honda, *Phys. Rev. B* **72**, 132103 (2005).
- <sup>14</sup>M. I. McMahon, L. F. Lundegaard, C. Hejny, S. Falconi, and R. J. Nelmes, *Phys. Rev. B* **73**, 134102 (2006).
- <sup>15</sup>Y. K. Vohra and P. T. Spencer, *Phys. Rev. Lett.* **86**, 3068 (2001).
- <sup>16</sup>Y. Akahama, H. Kawamura, and T. Le Bihan, *Phys. Rev. Lett.* **87**, 275503 (2001).
- <sup>17</sup>A. Brown and S. Rundqvist, *Acta Crystallogr.* **19**, 684 (1965).
- <sup>18</sup>J. C. Jamieson, *Science* **139**, 1291 (1963).
- <sup>19</sup>T. Sasaki, K. Shindo, K. Niizeki, and A. Morita, *J. Phys. Soc. Jpn.* **57**, 978 (1988).
- <sup>20</sup>I. Hamada, T. Oda, and N. Suzuki, in *Science and Technology of High Pressure, Proceedings of AIRAPT-17*, edited by M. H. Manghnani, W. J. Nellis, and M. F. Nicol (University Press, Delhi, India, 2000), Vol. 1, p. 467.
- <sup>21</sup>R. Ahuja, *Phys. Status Solidi B* **235**, 282 (2003).
- <sup>22</sup>S. Ostanin, V. Trubitsin, J. B. Staunton, and S. Y. Savrasov, *Phys. Rev. Lett.* **91**, 087002 (2003).
- <sup>23</sup>F. J. H. Ehlers and N. E. Christensen, *Phys. Rev. B* **69**, 214112 (2004).
- <sup>24</sup>T. Ishikawa, H. Nagara, K. Kusakabe, and N. Suzuki, *Phys. Rev. Lett.* **96**, 095502 (2006).
- <sup>25</sup>A. S. Mikhaylushkin, S. I. Simak, B. Johansson, and U. Häussermann, *Phys. Rev. B* **76**, 092103 (2007).
- <sup>26</sup>M. Marqués, G. J. Ackland, L. F. Lundegaard, S. Falconi, C. Hejny, M. I. McMahon, J. Contreras-García, and M. Hanfland, *Phys. Rev. B* **78**, 054120 (2008).
- <sup>27</sup>S. Endo, Y. Akahama, S. Terada, and S. Narita, *Jpn. J. Appl. Phys.* **21**, L482 (1982).
- <sup>28</sup>Y. Akahama and H. Kawamura, *J. Appl. Phys.* **100**, 043516 (2006).
- <sup>29</sup>Y. Akahama and H. Kawamura, *J. Phys.: Conf. Ser.* **215**, 012195 (2010).
- <sup>30</sup>Y. Ohishi, N. Hirao, N. Sata, K. Hirose, and M. Takata, *High Pressure Res.* **28**, 163 (2008).
- <sup>31</sup>O. Shimomura, K. Takemura, H. Fujihisa, Y. Fujii, Y. Ohishi, T. Kikegawa, Y. Amemiya, and T. Matsushita, *Rev. Sci. Instrum.* **63**, 967 (1992).
- <sup>32</sup>F. Izumi and T. Ikeda, *Mater. Sci. Forum* **321**, 198(2000).
- <sup>33</sup>A. K. Singh and C. Balasingh, *J. Appl. Phys.* **48**, 5338 (1978).
- <sup>34</sup>G. M. Sheldrick, *Acta Crystallogr. Sec. A* **64**, 112 (2008).
- <sup>35</sup>T. Kikegawa and H. Iwasaki, *Acta Crystallogr. Sec. B* **38**, 158 (1983).
- <sup>36</sup>H. Iwasaki, *Phys. Rev. B* **55**, 14645 (1997).
- <sup>37</sup>R. G. Greene, H. Luo, and A. L. Ruoff, *Phys. Rev. B* **51**, 597 (1995).
- <sup>38</sup>M. I. McMahon, O. Degtyareva, and R. J. Nelmes, *Phys. Rev. Lett.* **85**, 4896 (2000).
- <sup>39</sup>U. Schwarz, L. Akselrud, H. Rosner, Alim Ormeci, Yu. Grin, and M. Hanfland, *Phys. Rev. B* **67**, 214101 (2003).
- <sup>40</sup>Y. Sasa and M. Uda, *J. Solid State Chem.* **18**, 63 (1976).